

SPECTROSCOPY OF STELLAR JETS, OUTFLOWS, AND YOUNG STELLAR OBJECTS WITH THE *INFRARED SPACE OBSERVATORY*

A. Noriega-Crespo

SIRTF Science Center, California Institute of Technology, USA

RESUMEN

El *Observatorio Infrarrojo Espacial (ISO)* fue una misión europea muy exitosa, que nos ha dado una vista del Universo en el infrarrojo sin paralelo alguno, incluyendo cientos de observaciones de regiones de formación estelar y de flujos bipolares. Tres de los equipos instrumentales, a cargo de la cámara infrarroja (CAM) y los espectrómetros de longitudes de onda corta (SWS) y larga (LWS), usaron una fracción importante de su tiempo garantizado en el estudio espectroscópico de objetos y flujos estelares jóvenes. Aquí resumiré brevemente algunos de los hallazgos principales, en particular la detección de agua, las líneas rotacionales de H_2 y la presencia de otras moléculas más complejas. Presentaré nuevos resultados espectroscópicos de los flujos HH 1–2, HH 7–11 y Cep E, y de sus fuentes. Finalmente, discutiré algunas de las tendencias generales que se obtienen de estas observaciones, así como su importancia para entender la emisión de estos objetos usando modelos de choques J y C.

ABSTRACT

The *Infrared Space Observatory (ISO)* was an extremely successful European space mission that gave us an unparalleled view of the Universe in the infrared, and provided us with hundreds of observations of star forming regions and bipolar outflows. Three of the instrument teams, in charge of the infrared camera (CAM) and the two spectrometers at short and long wavelengths (SWS and LWS respectively), used a significant fraction of their guarantee time to study YSOs and outflows spectroscopically. In this contribution, I will briefly review some of their main findings, particularly the detection of water, H_2 rotational emission lines and the presence of other complex molecules. I will present new spectroscopic results on HH 1–2, HH 7–11 and Cep E, and their sources. And finally, I will discuss some of the general trends derived from these observations and their relevance in understanding the emission from these objects using J- and C-shock models.

Key Words: INFRARED: ISM — ISM: JETS AND OUTFLOWS — LINE: PROFILES — STARS: MASS LOSS — STARS: PRE-MAIN SEQUENCE

1. INTRODUCTION

After years of planning and development, the *Infrared Space Observatory (ISO)* was launched in November of 1995, carrying four state-of-the-art instruments and new mid/far-infrared detectors. Over the next two and a half years *ISO* provided us with a wealth of incredible observations and a revolutionary view of the infrared universe. It was the first time that we could look at mid/far infrared wavelengths with such sensitivity and angular resolution, and of course, it presented a great opportunity to advance our knowledge of star-forming regions and related objects. For the spectroscopic study of outflows, jets and their sources it provided the possibilities: (1) to determine the physical conditions of the atomic/ionic/molecular gas, (2) to describe in more detail their shock/ionization structure, (3) to understand the overall energy budget, (4) to study the relationship between the sources and the emitted

spectra from their outflows, and (5) to analyze the global trends provided by a larger sample of objects.

1.1. *ISO Instruments*

ISO had a 60-cm mirror and four instruments that were kept at temperatures of 2–8 K using a large cryo-vessel with over 2000 liters of superfluid Helium (Leech & Pollock 2000). A camera (ISOCAM), a photometer (ISOPHOT) and two spectrometers at short (SWS) and long (LWS) wavelengths were the four scientific instruments aboard *ISO*. Both ISOCAM and ISOPHOT also had spectroscopic capabilities, CAM with a Circular Variable Filter (CVF) mode, and PHOT with the Phot-S mode. The four instruments had a 3' unvignetted field of view (FOV). Some of the main characteristics of these instruments are the following. ISOCAM was a two channel camera with two InSb 32×32 arrays which covered wavelength ranges of approximately 2.3–5.1 μm (short) and 5.0–17.3 μm (long).

Each channel allowed four different magnifications (1.5, 3, 6 and 12"/pixel), and in the CVF mode had a spectral resolution $R = 40$ (Sibenmorgen et al. 1999). The Short Wavelength Spectrometer (SWS) covered the 2.38–45 μm wavelength range, with spectral resolutions from $R = 400$ (low resolution grating spectrum) to $R = 20,000$ (Fabry-Perot). It had different apertures depending on the wavelength region of the grating; at the short range $14 \times 20''$ (2.38–12 μm); at the long range $14 \times 27''$ (12–27.5 μm), $20 \times 27''$ (27.5–29 μm) and $20 \times 33''$ (29.0–45.2 μm). At least 4 different types of detectors were used in the grating mode: InSb (2.38–4.08 μm), Si:Ga (4.08–12.0 μm), Si:As (12.0–29 μm) and Ge:Be (37–48 μm) (Leech, de Graauw et al. 2000). The Long Wavelength Spectrometer (LWS) covered the wavelength range 43–196 μm , with spectral resolutions from $R = 200$ (medium resolution grating spectrum) to $R = 10,000$ (Fabry-Perot). It had a circular FOV of $\sim 80''$, and three different types of detectors were used: GeBe (43–50.5 μm), Ge:Ga (49.5–110 μm) and stressed Ge:Ga (103–196 μm) (Gry et al. 2000).

1.2. Key Programs on Star Formation, Outflows, Jets and their Sources

ISOCAM, SWS and LWS dedicated a substantial fraction of their guaranteed time to carry out spectroscopic observations of jets, outflows and their sources. The ISOCAM group led by S. Cabrit obtained nearly 100 observations in their project to study the mid-infrared emission associated with energetic bipolar outflows and the circumstellar dust halos around YSOs. One of the scientific goals of this project was to detect the [Ne III] 12.8 μm emission line, as an indicator of relatively high velocity shocks ($\geq 60 \text{ km s}^{-1}$), as well as to analyze the effect of the UV field created by such shocks on the nearby dust particles.

The programs ‘Pre-Main Sequence Stellar Evolution’ and ‘The Nature of YSOs’ of the LWS consortium were led by Paolo Saraceno. These programs obtained more than 200 observations, including several full grating SWS spectra as well, of objects such as classical T Tauri, Herbig Ae/Be and FU Orionis stars (Benedettini et al. 2000; Giannini et al. 1999; Lorenzetti et al. 1999, 2000; Nisini et al. 1999; Spinoglio et al. 2000).

The SWS team had several projects to study the nature and evolution of interstellar dust, both in the dense environment associated with molecular clouds and low mass protostars, as well as the dust associated with intermediate and massive young stars. Some of the topics studied by the researchers working with them (e.g., W. Van Dishoeck, D. Whittet,

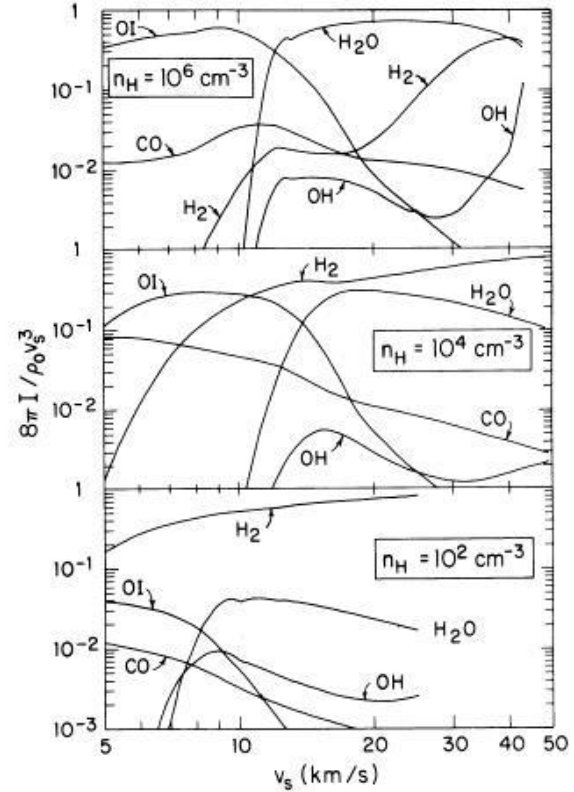


Fig. 1. Fractional cooling in MHD molecular shocks (C-shocks). At high densities and velocities H_2O , H_2 and [O I] dominate the overall cooling. Reproduced from Draine et al. (1983).

and P. Wasellius) explored different aspects of the gas-phase and solid (ices) chemistry of species such as H_2O and CO_2 , and the chemical state of molecules like OH, C_2H_2 , CH_3 , and CH_4 . Again, these programs obtained nearly 200 observations and have led to the publication of several articles, and at least two very complete PhD Theses by A. Boogert (“The Interplay between Dust, Gas, Ice and Protostars”) and M. van den Ancker (“Circumstellar Material in Young Stellar Objects”).

Besides these GTO projects, hundreds of observations in the Open Time were awarded to study problems of star formation and outflows. All the *ISO* data became public in December 1998, making available over 30,000 scientific observations, the result of approximately 1000 individual programs.

2. THERMAL WATER EMISSION

Among the most significant results obtained by *ISO* was the detection of water in active star forming regions. Theory had already predicted that in molecular shocks or magneto-hydrodynamic C-type shocks (Figure 1), at relatively high densities

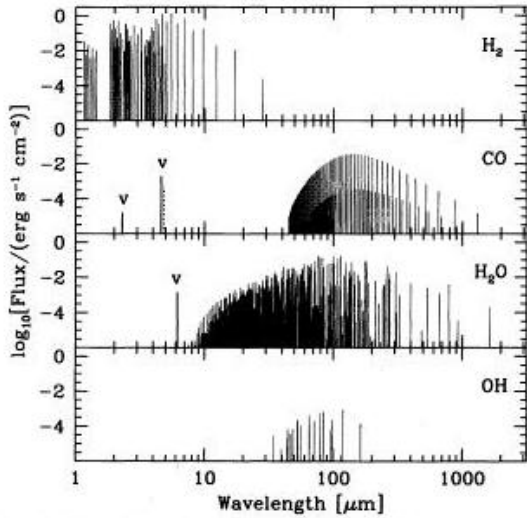


Fig. 2. Emission spectra from a MHD molecular shock (C-shock) at 40 km s^{-1} , $n(\text{H}_2) = 10^5 \text{ cm}^{-3}$, $B = 447 \mu\text{G}$ of the main molecular species from 1–2000 μm . Reproduced from Kaufman & Neufeld (1996).

(10^4 – 10^6 cm^{-3}), there was a range in velocity (15 – 40 km s^{-1}) in which water was the most important coolant (Draine, Roberge, & Dalgarno 1983). Under such conditions the shocks eroded ice mantles from the dust grains, returning the H_2O to its gas phase and making available several transitions to release the energy in the far infrared. One of the most striking examples of this process detected by *ISO* was HH 54 (Liseau et al. 1996), where LWS found 20 or more ortho and para water emission lines and such that $n(\text{H}_2\text{O})/n(\text{H}_2) = 10^{-5}$, i.e., an abundance higher than the expected value in quiescent molecular clouds (10^{-7} – 10^{-6}), and with a cooling comparable to the mechanical energy of the outflow ($10^{-2}L_\odot$).

Another important example was that of Orion BN-KL object (Harwit et al. 1998), where LWS Fabry-Perot observations detected 8 different transitions, with a water abundance of $n(\text{H}_2\text{O})/n(\text{H}_2) = 5 \times 10^{-4}$, in agreement with the latest theoretical models of the spectra (Figure 2) emitted by C-shocks (Kaufmann & Neufeld 1996).

3. HH 7–11 OUTFLOW

The bipolar outflow defined by the HH 7–11 system is one of the brightest and best studied. Its redshifted outflow lobe is invisible at optical wavelengths, so that the study of this object permits a comparison between the properties of embedded outflows and those of optical HH objects. We have recently analyzed the mid/far infrared physical char-

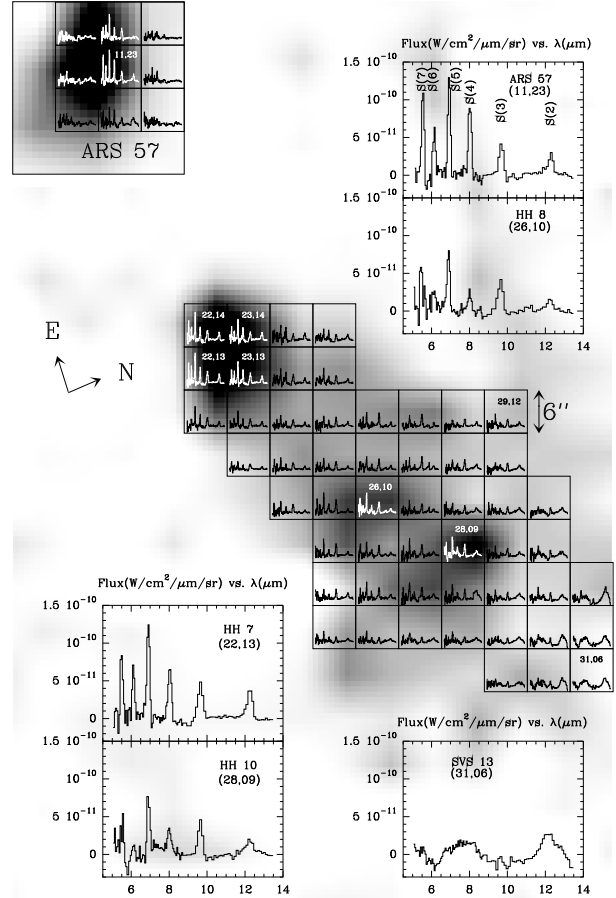


Fig. 3. ISOCAM CVF image of HH 7–11 at $\text{H}_2(0,0) 6.91 \mu\text{m}$ (continuum subtracted). The emission from this flow in the mid-IR is dominated by H_2 pure rotational lines. Spectra from individual knots are shown in detail. $\text{FOV} \sim 90''$.

acteristics of HH 7–11 using SWS and LWS observations (Molinari et al. 2000). We found atomic ($[\text{O I}] 63 \mu\text{m}$ and $145 \mu\text{m}$, $[\text{Si II}] 34.8 \mu\text{m}$) and molecular (H_2 , CO and H_2O) emission lines along the bipolar flow. Indeed, there was no significant difference in their properties between the optical and the invisible outflow component. We find that the emission could be explained by a combination of J and C-shocks with velocities of 20 – 50 km s^{-1} and preshock densities of 10^4 – 10^5 cm^{-3} . The SWS and LWS have a limited spatial resolution because of their apertures, and so the CVF ISOCAM observations of HH 7–11 provide further information on its emission properties. Figure 3 shows the outflow in the pure rotational line of $\text{H}_2 S(5)$ emission at $6.91 \mu\text{m}$ (a single data cube plane) together with the spectra obtained at each pixel, including HH 7, 8, and 10. We notice that (i) the spectra are dominated by the H_2 pure

rotational lines $S(7)$ through $S(2)$, (ii) that the morphology of the system is almost identical to that of the $H_2(1,0) S(1)$ emission at $2.12 \mu\text{m}$, and (iii) behind HH 10 close to the position of HH 11, there is a trace of $[\text{Ne II}] 12.8 \mu\text{m}$. This presence of $[\text{Ne II}]$ indicates J-shocks with velocities $\geq 60 \text{ km s}^{-1}$, a bit higher than that $40\text{--}50 \text{ km s}^{-1}$ inferred from optical spectroscopic measurements (Solf & Böhm 1990). The H_2 rotational lines are consistent with our previous findings (Molinari et al. 2000) of the excitation temperatures ($\sim 500\text{--}800 \text{ K}$) and column densities ($\sim 2\text{--}12 \times 10^{19} \text{ cm}^{-2}$) (Noriega-Crespo et al. 2001).

4. CEPHEUS E OUTFLOW

Cep E is another example of an embedded/optical outflow. A bright knot in the southern outflow lobe is visible in $H\alpha$ and $[\text{S II}] 6717/31$, and known as HH 337. Some of the interesting characteristics of Cep E is that it appears to be driven by an unique Class 0 protostar (Lefloch, Eislöffel, & Lazareff 1996), and the outflow itself is very young, with a dynamical age of $\sim 3000\text{--}5000$ years. Cep E was observed with ISOCAM CVF and LWS in full grating mode, and we have recently analyzed these observations (Moro-Martín et al. 2001). Figure 4 shows the CVF image in the $S(5) (0,0)$ emission at $6.91 \mu\text{m}$, with the spectrum at each pixel. We notice that both outflow lobes are dominated by H_2 pure rotational emission lines, and *surprisingly* the IRAS 230111+6126 source is detected. We also find that this emission is remarkable similar to that at $2.12 \mu\text{m}$ (Eislöffel et al. 1996; Ayala et al. 2000). In this case, we found $T_{\text{ex}} \sim 950\text{--}1300 \text{ K}$ and $N(\text{H}_2) \sim 1\text{--}3 \times 10^{19} \text{ cm}^{-2}$, i.e., somewhat higher temperatures and smaller column densities than in HH 7–11.

The LWS spectrum of the North and South outflow lobes show more than 20 molecular lines of CO, H_2O and OH (Figure 5). From the CO, H_2O , and H_2 cooling, we determine that the FIR spectra was generated by C-shocks with speeds of $20\text{--}30 \text{ km s}^{-1}$. The $[\text{O I}] 63 \mu\text{m}$ and $[\text{C II}] 158 \mu\text{m}$ fine-structure emission lines were also detected with similar strengths, indicating contamination by photodissociation in the $[\text{C II}]$ line. In order to explain the corrected $[\text{O I}] 63 \mu\text{m}$ collisionally excited line, J-shocks with speeds of $\sim 20\text{--}30 \text{ km s}^{-1}$ are required. Water was overabundant by factors of $10^2\text{--}10^3$, i.e., consistent with the low excitation and youth of Cep E.

5. HH 1–2 OUTFLOW

The bright and well-studied HH 1–2 system was also observed by *ISO* with SWS medium resolution,

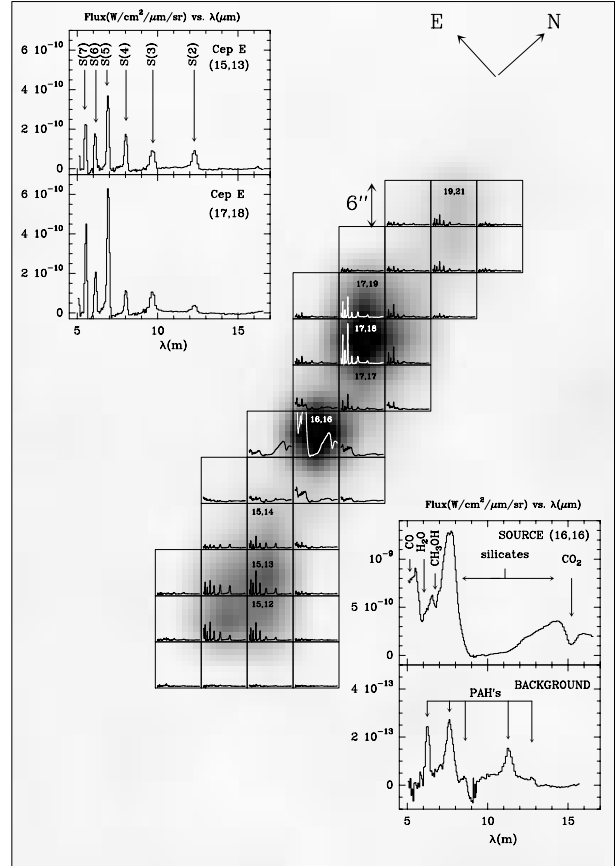


Fig. 4. ISOCAM CVF image of Cep E at $H_2(0,0) 6.91 \mu\text{m}$. The emission from this flow in the mid-IR is dominated by H_2 pure rotational lines. Spectra from individual knots are shown in detail. FOV $\sim 90''$.

LWS full grating, and CAM CVF. We are in the process of analyzing these data (see e.g., Cenicharo et al. 1999). Unlike HH 7–11 or Cep E, the HH 1–2 objects are *high excitation* objects (Figure 6), i.e., with shock velocities of $\sim 100 \text{ km s}^{-1}$, enough to produce high ionization $[\text{O III}] \lambda 5007$ emission. Unfortunately the observations of HH 1 have been “contaminated” by the bright Cohen-Schwartz source that lies nearby along the outflow. The H_2 pure rotational lines $S(7)$ through $S(1)$ were observed by SWS, as well as $[\text{Si II}] 34.8 \mu\text{m}$. CAM CVF detected the $H_2(0,0) S(2)\text{--}S(7)$ lines, but also in some knots (HH 2H) $[\text{Ne II}] 12.8 \mu\text{m}$ and $[\text{Ne III}] 15 \mu\text{m}$, indicating $v_{\text{shock}} > 60 \text{ km s}^{-1}$ (Figure 7). The LWS spectra were taken at 3 positions (HH 1, 2 and VLA 1 source) and no molecular lines of CO, H_2O , and OH were detected. The fine structure atomic lines of $[\text{O I}] 63 \mu\text{m}$ and $[\text{C II}] 158 \mu\text{m}$ are clearly seen and with a similar brightness. This suggests a strong photodissociation component due to the surrounding UV field that affects the strength of the $[\text{C II}]$ line.

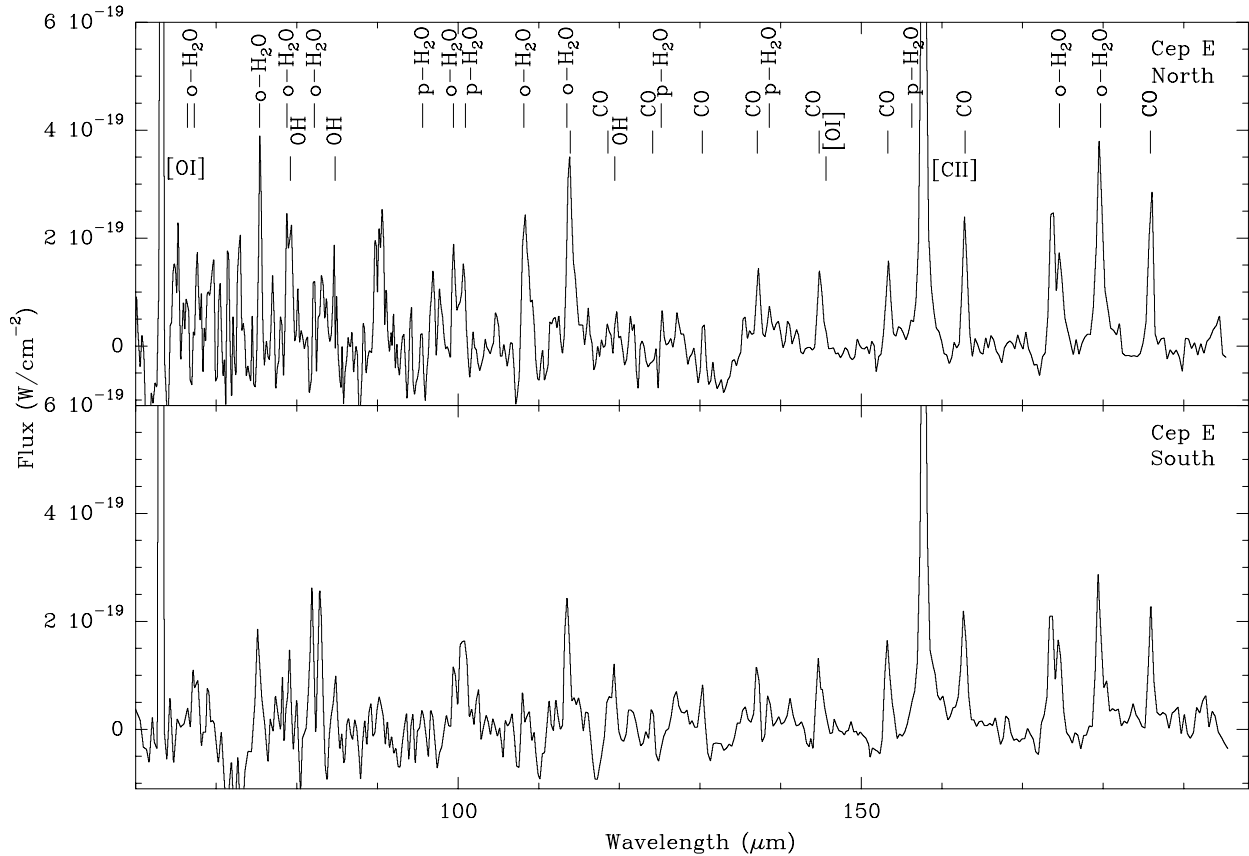


Fig. 5. Full grating LWS spectra of Cep E North and Cep E South. The spectra are rich in CO, H₂O and OH emission lines. [O I] 63 μm and [C II] 158 μm are detected and are equally strong.

Emission Lines from Jet Flows (Isla Mujeres, Q.R., México, November 13-17, 2000)
Editors: W. J. Henney, W. Steffen, A. C. Raga, & L. Binette

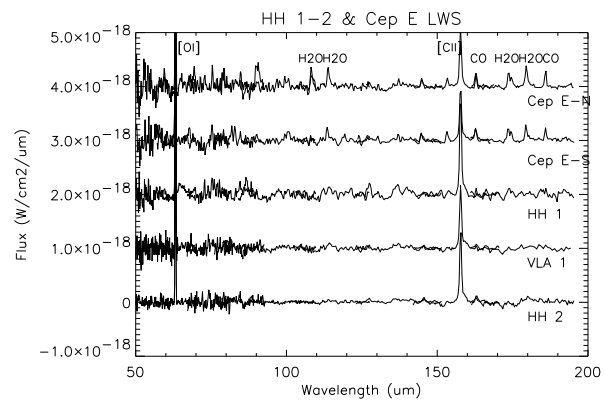


Fig. 6. A comparison of the HH 1-2 and Cep E outflows in the FIR, which stresses the difference between a high-excitation optically visible object (HH 1-2) and a low-excitation embedded one (Cep E).

6. CLASS 0/I SOURCES

A very nice result from the *ISO* observations came from the CAM CVF observations towards Class 0 sources. A Class 0 source, by definition, is a true protostar with the peak of its spectral energy distribution at sub-mm or FIR wavelengths. They are deeply embedded inside an “envelope”, detected in many cases thanks to their powerful bipolar outflows. Our first CAM observations of Cep E detected, *at mid infrared wavelengths*, the driving source (Noriega-Crespo, Garnavich, & Molinari 1998), presumably a Class 0 source. The CVF observations confirmed this detection and displayed a series of spectral absorption features between 5–17 μm (CH₄ at ~ 7.5 μm, Silicates at 9–10 μm, and CO₂ at 14–15 μm) closer to those expected from a more evolved Class I source. We found a similar result for the VLA 1 source in the HH 1–2 outflow and other well known Class 0 sources, like NGC1333-IRAS2 or L1448-N (Cernicharo et al. 2000). The difference with respect to a source like IRAS230111+6126, is that the absorption features

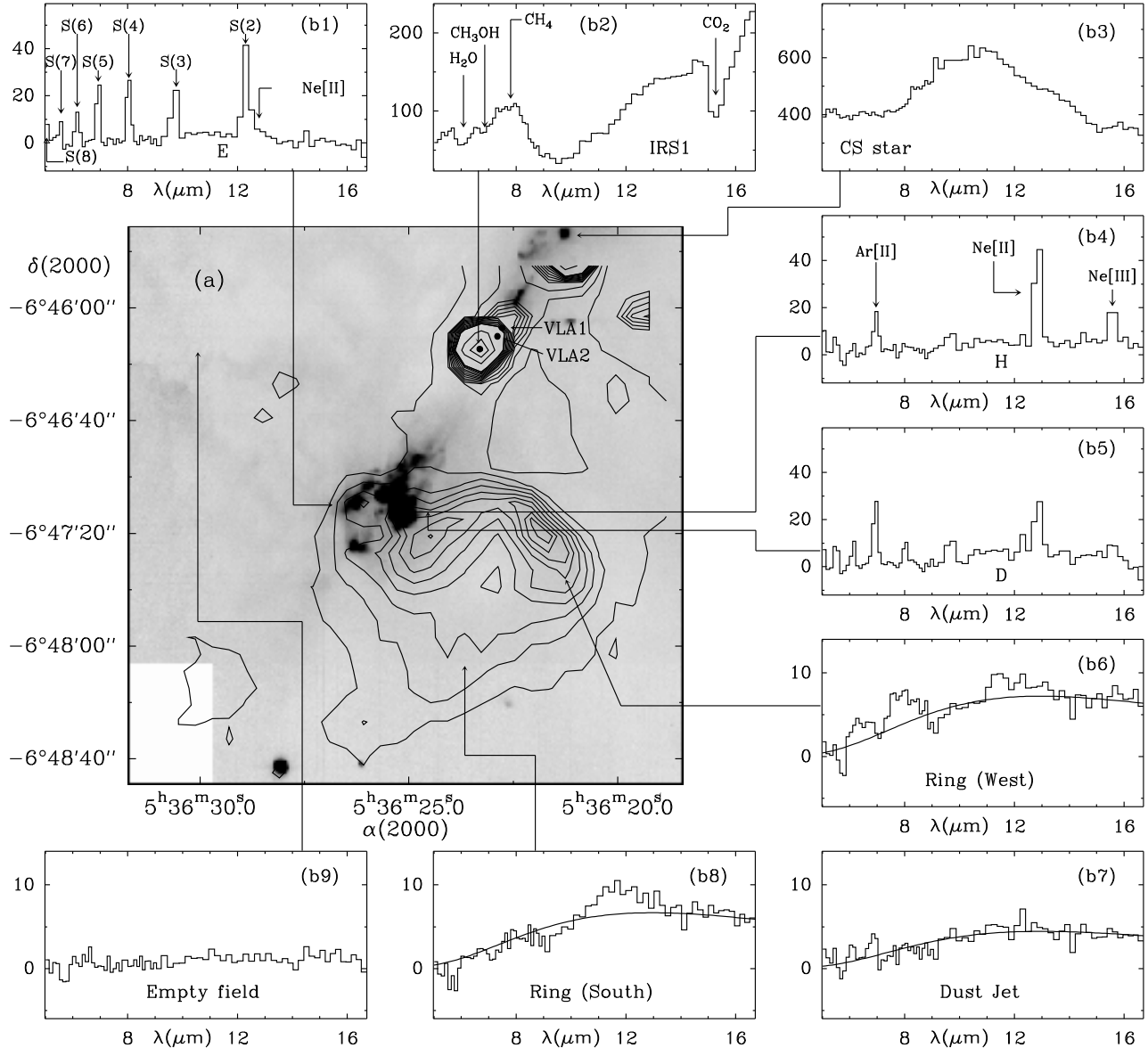


Fig. 7. ISOCAM CVF (4–17 μm) image of HH 2 and VLA 1 region (reproduced from Cernicharo et al. 1998). The emission of HH 2 contains H_2 (0,0) rotational lines as well as $[\text{Ne II}]$ 12.8 μm and $[\text{Ne III}]$ 14.5 μm lines. Dust emission from the jet is also detected.

are so deep, that what is left in the mid-IR SED are a series of emission windows at ~ 5.3 , 6.6 & 7.5 μm (see Figure 8). In the case of VLA 1, for instance, we can reproduce the mid-IR SED with an object of size 4 AU at 700 K and with an extinction of $A_V = 80$ –100 magnitudes (soft line in Fig. 8).

7. GENERAL TRENDS: EXAMPLES

7.1. Cooling from C-shocks

When the *ISO* data archive became public in December 1998, it was clear that one could have access to a large sample of objects and hence be

able to ask more global questions about the behavior and energetics of outflows, jets and their sources. An example of this approach was carried out by P. Saraceno and his group based on LWS observations of Class 0–III sources (Saraceno et al. 1998). In Figure 9 we used a similar idea (see, e.g., Spigolino et al 2000) to determine the shock velocity in a series of outflows, based on their H_2O , $[\text{O I}]$ 63 μm and CO cooling when compared with the predictions from C-type shocks (Draine et al. 1983; Kaufmann & Neufeld 1996). To a first approximation the cooling from these species defines a narrow

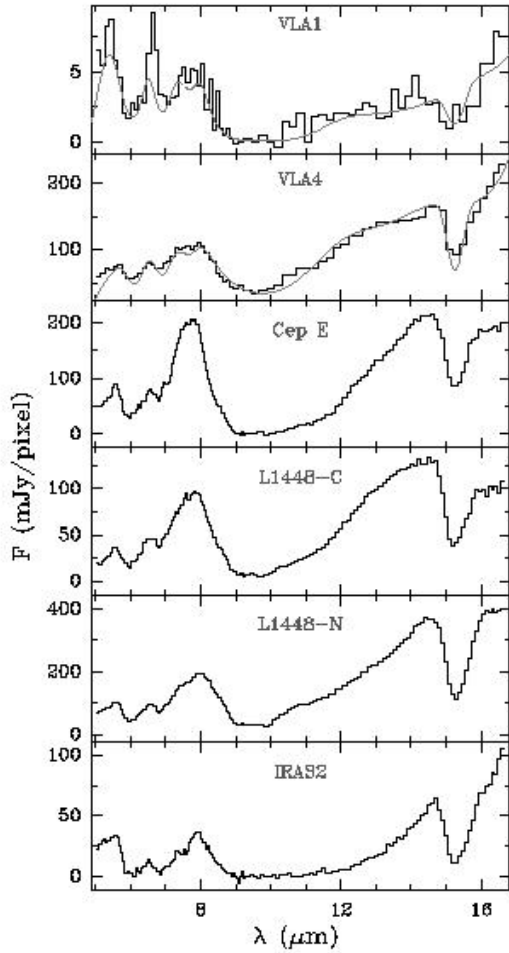


Fig. 8. A sample of Class 0/I sources showing their similarity at mid-IR wavelengths (from Cernicharo et al. 2000)

range of shock velocities ($10\text{--}20\text{ km s}^{-1}$) and densities ($\log n(\text{H}_2) = 4.5\text{--}5.5$), with perhaps a couple of exceptions (IC1396N and IRAS 16293). If we approximate the working surfaces of the jets/outflows by bowshocks, then the above result suggests that the molecular emission arises away from the stagnation region, further “downstream” and along the bowshock wings. A result compatible with the numerical hydrodynamic simulations of working surfaces, with parallel integrated chemistry (Williams 2002; Lim, Rawlings, & Williams 1999).

7.2. H_2O from Circumstellar Envelopes

LWS observations have recently been used (Cecarelli et al. 1999) to study the correlation between H_2O thermal emission arising from protostellar sources and their 1.3-mm continuum fluxes or SiO millimetric emission. The idea is to try to

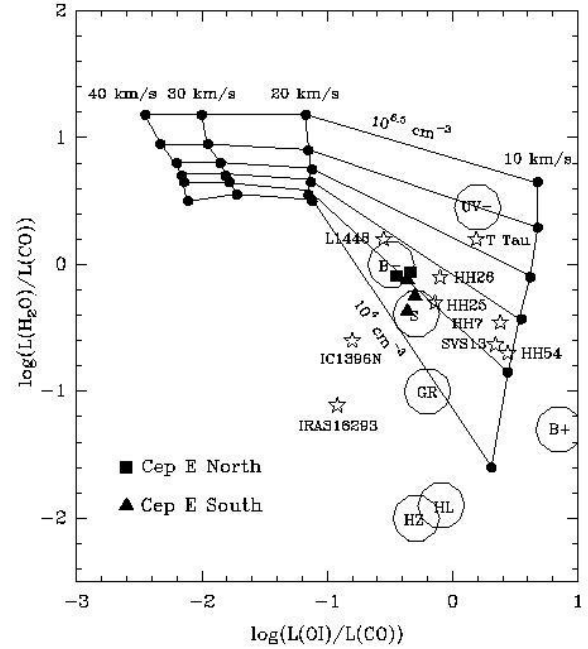


Fig. 9. The molecular cooling at FIR wavelengths from several outflows, observed with LWS, compared with the predictions from C-shock models.

distinguish if the H_2O emission comes from the outflows (SiO as a tracer) or if it is found closer to the source (an envelope, with 1.3-mm flux as a tracer). Although the results are far from conclusive (see, e.g., Neufeld et al. 2000), from a sample of 7 YSOs, 5 seem to correlate quite well with their 1.3 mm fluxes (Figure 10), but not with the SiO emission. The suggested explanation is that the H_2O lines originate from the warm inner region of an infalling envelope, with accretion rates of a few $10^5 M_\odot \text{ yr}^{-1}$.

8. SUMMARY

Astronomically *ISO* was a very successful mission, and for star forming regions, stellar jets, outflows and their sources, it meant hundreds of new observations at mid and far infrared wavelengths. I have shown a small sample of the spectroscopic results on some prototypical outflows, such as HH 1–2, HH 7–11 and Cep E, that have illustrated the different *ISO* observational modes and the physical conditions that can be derived from them. It is clear that molecular cooling at FIR wavelengths is an important component of the overall energy budget of outflows and jets. One of the nice surprises from *ISO* has been the possibility to observe deeply embedded sources at mid-IR wavelengths, since this opens a door for ground-based observations with large telescopes of some of the lesser known phases of the star formation process.

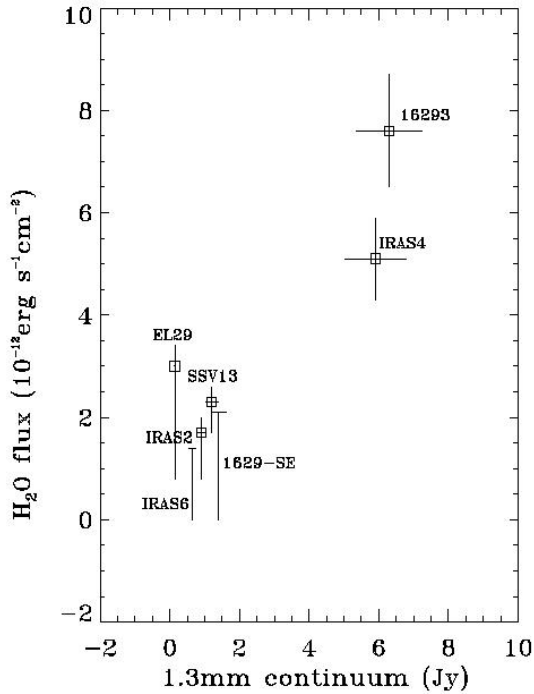


Fig. 10. H_2O thermal emission from a sample of YSOs compared with their 1.3-mm fluxes (from Ceccarelli et al. 1999).

It is a pleasure to thank A. Raga and L. Binette for their warm welcome and the great organization of this meeting. It is also a pleasure to thank my collaborators: B. Ali, S. Cabrit, C. Ceccarelli, J. Cernicharo, S. Molinari, A. Moro-Martín, P. Saraceno, A. Sargent, and L. Testi. Thanks to the SOC for the invitation. Last, but not least, thanks to J. Cantó, A. Frank, J. A. López, A. Raga, and J. M. Torrelles for enlightened conversations, and *gracias* to A. Moro-Martín for her careful reading of this manuscript.

REFERENCES

- Ayala, S., Noriega-Crespo, A., Garnavich, P., et al. 2000, *AJ*, 120, 909
- Benedettini, M., et al. 2000, *A&A*, 359, 148
- Ceccarelli, C., et al. 1999, *A&A*, 342, L21
- Cernicharo, J., Cesarsky, D., Noriega-Crespo, A., Lefloch, B. & Moro-Martín 1999 in *H₂ in Space*, eds. F. Combes, & G. Pineau des Forêts (Cambridge: CUP), 23
- Cernicharo, J., Noriega-Crespo, A., Cesarsky, D., et al. 2000 *Science*, 288, 649
- Draine, B. T., Roberge, W. G., & Dalgarno, A. 1983, *ApJ*, 264, 485
- Eisloffel, J., Smith, M. D., Davis, C. J., & Ray, T. P. 1996, *AJ*, 112, 2086
- Giannini, T., et al. 1999, *A&A*, 346, 617
- Gry, C., et al. 2000, *The ISO Handbook*, Vol IV, 14
- Harwit, M., Neufeld, D. A., Melnick, G. J., & Kaufman, M. J. 1998, *ApJ*, 497, L105
- Kaufman, M. J., & Neufeld, D. A. 1996, *ApJ*, 456, 611
- Leech, K., de Graauw, Th., et al. 2000, *The ISO Handbook*, Vol VI, 16
- Leech, K., & Pollock, A. M. T. 2000, *The ISO Handbook*, Vol II, 3
- Lefloch, B., Eisloffel, J., & Lazareff, B. 1996, *A&A*, 313, L17
- Lim, A. J., Rawlings, J. M. C., & Williams, D. A. 1999, *MNRAS*, 308, 1126
- Liseau, R., Ceccarelli, C., Larson, B., et al. 1996, *A&A*, 315, L181
- Lorenzetti, D., et al. 1999, *A&A*, 346, 604
- Lorenzetti, D., et al. 2000, *A&A*, 357, 1035
- Molinari, S., Noriega-Crespo, A., Ceccarelli, C., et al. 2000, *ApJ*, 538, 698
- Moro-Martín, A., Noriega-Crespo, A., Molinari, S., Testi, L., Cernicharo, J., & Sargent, A. 2001, *ApJ*, 555, 146
- Nisini, B., et al. 1999, *A&A*, 350, 529
- Noriega-Crespo, A., Garnavich, P., & Molinari, S. 1998, *AJ*, 116, 1388
- Noriega-Crespo et al. 2002, in preparation
- Neufeld, D. A., et al. 2000, *ApJ*, 539, L107
- Saraceno, P., et al. 1998 in *Star Formation with ISO*, ASPCS, 132, 233
- Siebenmorgen, R., Blommaert, J., Sauvage, M., & Starck, J-L. 1999, V III, p4
- Spinoglio, L., et al. 2000, *A&A*, 353, 1055
- Solf, J. & Bohm, K-H. 1990, *ApJ*, 348, 297
- Williams, D. A. 2002, *RevMexAA(SC)*, 13, 114 (this volume)